Cosmic slowing down of acceleration with the Chaplygin-Jacobi gas as a dark fluid?

J.A.S.Fortunato,[1, 2, 3, ∗] W.S. Hipólito-Ricaldi,[4, 2, †] N. Videla,[5, ‡] and J.R. Villanueva[6, §]

[1]*PPGCosmo, CCE, Universidade Federal do Espírito Santo,*
Av. Fernando Ferrari, 540, CEP 29.075-910, Vitória, ES, Brazil
[2]*Núcleo Cosmo-UFES, CCE, Universidade Federal do Espírito Santo,*
Av. Fernando Ferrari, 540, CEP 29.075-910, Vitória, ES, Brazil
[3]*Instituto Argentino de Radioastronomía, C.C. No. 5, 1894 Buenos Aires, Argentina*
[4]*Departamento de Ciências Naturais, CEUNES, Universidade Federal do Espírito Santo,*
Rodovia BR 101 Norte, km. 60,CEP 29.932-540, São Mateus, ES, Brazil
[5]*Instituto de Física, Pontificia Universidad Católica de Valparaíso,*
Avenida Universidad 331, Curauma, Valparaíso, Chile
[6]*Instituto de Física y Astronomía, Facultad de Ciencias, Universidad de Valparaíso,*
Avenida Gran Bretaña 1111, Playa Ancha, Valparaíso, Chile

A particular generalization of the Chaplygin inflationary model, using the formalism of Hamilton-Jacobi and elliptic functions, results in a more general non-linear Chaplygin-type equation of state (Chaplygin-Jacobi model). We investigate the implementation of this model as a dark energy (DE) fluid to explain the recent acceleration of the universe. Unlike ΛCDM and other Chaplygin-like fluids, where the final fate of the universe is an eternal de Sitter (dS) phase, the dynamics of this model allows for the possibility of a decelerating phase in the future, following the current accelerating phase. In other words, a transient acceleration arises, accounting for the recently claimed slowing down phenomenon. This Chaplygin-Jacobi model shows important differences compared to the standard and generalized Chaplygin gas models. Additionally, we perform a Markov Chain Monte Carlo (MCMC) analysis using several datasets, including Type Ia Supernovae (SNIa), Cosmic Chronometers (CC), Fast Radio Bursts (FRBs), and Baryon Acoustic Oscillations (BAO) to examine the observational viability of the model. Our results indicate that, although a transient phase of accelerated expansion is supported by current observations in the context of the Chaplygin-Jacobi model, this model is strongly disfavored in comparison with ΛCDM.

I. INTRODUCTION

One of the greatest challenges in modern science is understanding the universe, particularly its origin, evolution, and final fate. In this regard, the hot big bang (HBB) cosmology, based on four-dimensional General Relativity (GR) [1], has been widely accepted as the standard paradigm describing how the universe expanded from an initial singularity. During the longest part of its lifetime, the universe has undergone a decelerating expansion, being dominated first by radiation and then by matter. However, the cosmic history includes two phases of accelerated expansion: one at very early times and another at late times. The first accelerating phase corresponds to inflation, which supplies an explanation of the observed large scale structure (LSS), as it provides the primordial, almost adiabatic and scale-invariant perturbations that undergo gravitational collapse to form galaxies and clusters of galaxies [2]. The second accelerating phase corresponds to the current cosmic acceleration, which is supported from a large number of observational evidence [3–8], which also indicates that our universe is spatially almost flat, and currently dominated by dark energy (DE) and cold dark matter (DM). The accelerated expansion of the present universe is attributed to DE, which is an exotic component having negative pressure, such as the cosmological constant Λ [9–11]. The ΛCDM model, has proven to be successful in explaining a wide range of cosmological observations [3–8]. Despite its success, it faces several challenges, namely: (i) the cosmological constant problem [12, 13], (ii) the cosmic coincidence problem (or the so-called "why now" problem) [14, 15], and more recently, (iii) the tension between measurements of the Hubble parameter H_0 [16, 17] and (iv) the S_8 tension ($S_8 = \sigma_8 \sqrt{\Omega_m/0.3}$) [18].

Several approaches have been proposed to address ΛCDM problems. They generally fall into two groups: one modifies GR, while the other, dynamical DE, involves models where the properties of DE vary over time unlike in the ΛCDM. Several candidates for dynamical DE have been studied in recent years including the Chaplygin gas (CG). For a review of DE models, see Refs. [19–23]. The CG's equation of state (EoS) has a connection with string and brane theories [24, 25] and it can admit a supersymmetric generalization [26]. Chaplygin cosmology can be understood as the study of the dark sector through a CG fluid that satisfies the relation $p = -\frac{B}{\rho}$ [27–29], and its generalizations, like the Generalized Chaplygin Gas (GCG) with an equation of state $p = -\frac{B}{\rho^\alpha}$ [24, 30], where p represents pressure (assumed to be negative to produce an accelerated stage at late times), ρ

is the energy density, and B is a positive constant (to ensure $p < 0$) and $0 < \alpha \leq 1$. These models belong to the unified models class, which provide a description of the matter-dominated era and the late accelerating era with only one component rather than two (for other unified models, see e.g. [31–33]). However, observationally, the CG model has shown problems with instabilities in their corresponding trajectories [34] and when tested with various observations, such as Type Ia Supernovae (SNIa) , X-ray gas mass fraction of clusters, and Hubble rate-redshift data [35–39]. Moreover, although the GCG model is in agreement with background observational data [35–40], it suffers from an unexpected blow-up in the matter power spectrum caused by adiabatic pressure perturbations [41]. This undesired effect can be avoided if some kind of non-adiabaticity is introduced in the model (see e.g. [42]). Moreover, in recent years, several GCG modifications or generalizations have been proposed to study the dark sector. Among others, some of them are the modified Chaplygin gas (MCG) [43, 44], the new generalized Chaplygin gas (NCG) [45], and viscous generalized Chaplygin gas (VGCG) [46, 47]. For recent observational results involving those models, see e.g. [48].

Recently, a further generalization has been proposed through the Hamilton-Jacobi formalism in the inflationary context by means of elliptic functions [49]. This leads to the development of a more general Chaplygin-like EoS, which we will refer to as Chaplygin-Jacobi Gas model (CJG). The CJG EoS is expressed as follows:

$$p = -\frac{B\,k}{\rho^\alpha} - k'\rho\left(2 - \frac{1}{B}\rho^{\alpha+1}\right).$$

In the above equation, k represents the modulus of the elliptic function, and $k' = 1 - k$ is the complementary modulus. It is noteworthy that the GCG is obtained with $k = 1$ and $B > 0$. In recent years, the CJG has been studied in contexts different from this work [49–55].

Considering that Chaplygin-like fluids offer an interesting framework to study phenomenology beyond the ΛCDM, the main goal of the present work is to explore the viability of the CJG for describing the late universe. First, we integrate the balance equation and find its solutions for the energy density, pressure and EoS parameter. Then, we perform an analysis of its parameter space to find the region in which physical solutions are possible. After obtaining an analytical solution for the Hubble rate, and in order to compare the background evolution of the CJG with that of the ΛCDM model, we introduce parameters where derivatives of the scale factor beyond the second-order appear. To this end, one option is to study the so-called statefinder parameters, r and s, defined as follows [56, 57].

$$r \equiv \frac{\dddot{a}}{aH^3}, \tag{2}$$

$$s \equiv \frac{r - 1}{3(q - \frac{1}{2})}, \tag{3}$$

where the dot denotes differentiation with respect to cosmic time t, $H = \dot{a}/a$ represents the Hubble rate, and $q = -\ddot{a}/(aH^2)$ denotes the deceleration parameter. It is worth noting that the statefinder parameters involve third derivatives of the scale factor with respect to cosmic time, in contrast to the Hubble rate and the deceleration parameter, which are expressed in terms of the first and second time derivatives of the scale factor, respectively. Statefinder analysis serves as a diagnostic tool for understanding the dynamics of the universe's expansion. These parameters are computed for our specific DE model, and as we will discuss later, r and s can differ significantly from ΛCDM even if they predict very similar expansion histories.

While the emergent cosmology may not realize a unified model like most of the CG-like models, it offers a phenomenology with interesting results distinct from those of the CG model and its generalizations, particularly in future times. As is expected for any DE model, a fluid satisfying the relation (1) is subdominant in a multi-component universe during early times. This accurately reproduces a radiation-dominated era followed by a matter-dominated era, resulting in a decelerating universe. Subsequently, the DE fluid dominates, leading to an accelerating phase. However, a specific region in the parameter space permits a transient acceleration-deceleration in the future, indicating the possibility of a decelerating phase following the current accelerating phase. This phenomenon is commonly referred to as the *cosmic slowing down* of the current acceleration. DE models with a constant EoS like ΛCDM or the wCDM cannot exhibit the slowing down feature [58], as they predict a de Sitter (dS) phase as the final fate of the universe. However, depending on the set of parameters, some DE models, especially those with dynamical EoS or parametrizations like the Chevallier-Polarski-Linder (CPL) model and others, allow for this possibility (see e.g. [58–62]). Here, we demonstrate that a universe with a fluid satisfying the relation (1) as DE can also exhibit the slowing down behavior. Additionally, we conduct a data analysis to investigate whether recent astronomical and cosmological observations support this transient behavior in the context of the CJG. To achieve this, we utilize the latest supernova Pantheon + data (PAN$^+$), Cosmic Chronometers data (CC) and BAO data. Furthermore, we incorporate observations from Fast Radio Bursts (FRBs) into our tests, as they have recently been shown to provide an interesting complement to other cosmological probes.

Our work is organized as follows: after this introduction, in Section II, we derive solutions for the energy density, pressure, and EoS parameter. Next, we conduct an analysis of the parameter space to determine the sub-regions where physical solutions are feasible and the sub-regions where the slowing down phenomenon appears. In Section III, we delve into the background

cosmological dynamics of the CJG in a multifluid context. This includes obtaining an analytical solution for the Hubble rate $H(z)$ as a function of redshift and introducing the deceleration and Statefinder parameters tailored for the CJG. In Section IV, we present the data and relevant equations for the implementation of the MCMC analysis. In Section V, we present the results of the MCMC analysis and evaluate numerically the cosmic evolution of the CJG against redshift, comparing these results with those of the ΛCDM model. Finally, we summarize our findings and present our conclusions in Section VI. Throughout our work, we adopt the mostly positive metric signature $(-,+,+,+)$ and utilize natural units where $c = \hbar = 1$.

II. CHAPLYGIN-JACOBI DARK ENERGY

As mentioned before, the Hamilton-Jacobi formalism allows for obtaining a particular generalization of the Chaplygin inflationary model through elliptical functions, resulting in a more general Chaplygin-like EoS parameter [49]

$$\omega = -\frac{B\,k}{\rho^{\alpha+1}} - 2k' + \frac{k'}{B}\rho^{\alpha+1}, \tag{4}$$

where $k' = 1 - k$, and α, B and k are constants with $0 < k < 1$ and $0 < k' < 1$. In principle, the EoS in (1) reduces to a GCG case when $k = 1$, $B > 0$ and $0 < \alpha < 1$. The case where $B > 0$, $k = 1$ and $\alpha = 0$ reproduces ΛCDM. There is no other case in which one can obtain the MGC, NGC, or another Chaplygin-like EoS. In the GCG context, only the first term in Eq. (1) appears. Then, for $B > 0$ and $0 < \alpha < 1$, the pressure is always negative, allowing an explanation for the late accelerated expansion of the universe. However, the CJG has two additional contributions to the pressure. The second term of Eq. (1) is always negative, but the first and third terms always have opposite signs. For instance, for $B > 0$, the first term is negative and the third term is positive, while for $B < 0$ the behaviour is reversed. Eventually, depending on the parameter space, the positive term might dominate and the pressure might become less negative opening the the possibility of a slowing down of the cosmic acceleration. This becomes more evident when looking at the energy density and pressure as functions of the scale factor. Let us first consider one universe dominated by a fluid with an EoS as in Eq. (1) and solve the energy balance equation.

In the context of a universe described by the Friedman-Lemaître-Robertson-Walker (FLRW) metric, the energy balance equation for an EoS given by Eq. (1) reads

$$\frac{\dot{\rho}}{\rho} = -3\frac{\dot{a}}{a}\left(-\frac{B\,k}{\rho^{\alpha+1}} + 2k - 1 + \frac{(1-k)}{B}\rho^{\alpha+1}\right) = -3\frac{\dot{a}}{a}\left(\frac{-Bk - (1-2k)\rho^{\alpha+1} + \frac{1-k}{B}\rho^{2(\alpha+1)}}{\rho^{\alpha+1}}\right), \tag{5}$$

where a is the scale factor of the homogeneous and isotropic metric, and a dot denotes differentiation with respect to cosmic time. This equation can be integrated directly resulting in

$$\rho(a) = \left[B - \frac{BA}{Ak' - a^{3(1+\alpha)}}\right]^{\frac{1}{1+\alpha}}, \tag{6}$$

where A is an integration constant. It should be noted that a particular choice of parameters B, k and α does not uniquely determine the CJG model, as it is also necessary to specify the value of ρ at a particular redshift. This can be addressed by introducing $B = \rho_0^{(1+\alpha)}B_s$, where $\rho_0 = \rho(a_0) > 0$ is the current density. This ensures that the choice of B_s, k and α uniquely specifies the CJG model, and Eq. (6) can be conveniently rewritten as

$$\rho(a) = \rho_0\left[B_s - \frac{B_sA}{Ak' - a^{3(1+\alpha)}}\right]^{\frac{1}{1+\alpha}}, \tag{7}$$

where the integration constant A is determined by the condition $\rho = \rho_0$ at the present time, so that

$$A = \frac{1 - B_s}{1 - k(1 - B_s)}, \tag{8}$$

and thus,

$$\rho(a) = \rho_o\left[B_s - \frac{B_s(1 - B_s)}{(1 - B_s)k' - (k' + B_s\,k)a^{3(1+\alpha)}}\right]^{\frac{1}{1+\alpha}}. \tag{9}$$

Notice that the energy density spans a three-dimensional parameter space. Accordingly, the pressure of the CJG as a function of the scale factor can be computed by replacing Eq. (9) into Eq. (1). Although, in principle, solution (9) has a three-dimensional parameter space

$$\mathscr{M} = \{(\alpha, B_s, k)/\, \alpha \in \mathbb{R}, B_s \in \mathbb{R}, 0 < k < 1\}, \tag{10}$$

some regions of this space can lead to singularities, divergences in the past, or negative densities, resulting in non-physical solutions across the entire space $\mathcal{M}$. However, certain sub-regions of $\mathcal{M}$ allow solutions without these problems. Let us find the sub-regions in $\mathcal{M}$ where we can have physical solutions for the model.

A. Physical solutions

From a physical standpoint, we impose that the energy density must always be positive and that there are no singularities within the interval $0 < a < 1$. For convenience, it is better to analyze two different regimes for the parameter α: (i) $\alpha + 1 < 0$ and (ii) $\alpha + 1 \geq 0$. Let us analyze each case separately

1. Case $1 + \alpha < 0$

For $1 + \alpha = -|1 + \alpha| < 0$, the energy density in Eq. (9) can be rewritten as

$$\left(\frac{\rho}{\rho_0}\right)^{|1+\alpha|} = \frac{1}{B_s} \frac{1 + (B_s - 1)(k + k'a^{3|1+\alpha|})}{1 + (B_s - 1)k(1 - a^{3|1+\alpha|})}. \tag{11}$$

In that case, a singularity happens for

$$a_c^{3|1+\alpha|} = 1 + \frac{1}{k(B_s - 1)}. \tag{12}$$

To avoid any singularity in $0 < a < 1$, a_c must be outside of this interval. One possibility is to have $a_c^{3|\alpha+1|} \in \mathbb{R}$ and $a_c > 1$. This condition is possible only if the second term in Eq. (12) is always positive, i.e., for $B_s > 1$. Therefore, we have the first sub-region with physical solutions

$$\mathcal{N}_1 = \{(\alpha, B_s, k)/\alpha < -1, B_s > 1, 0 < k < 1\}. \tag{13}$$

Another possibility is that $a_c^{3|\alpha+1|} \notin \mathbb{R}$ and $a_c < 0$. This occurs only when $-\frac{k'}{k} < B_s < 1$. Nevertheless, in the past, when $a \ll 1$, we have the limit

$$\left(\frac{\rho}{\rho_0}\right)^{|1+\alpha|} \to \frac{1}{B_s}, \tag{14}$$

so, we discard negatives values for B_s, identifying another sub-region $\mathcal{N}_2 \subset \mathcal{M}$ with physical solutions, such that

$$\mathcal{N}_2 = \{(\alpha, B_s, k)/\alpha < -1, 0 < B_s < 1, 0 < k < 1\}. \tag{15}$$

2. Case $\alpha + 1 \geq 0$

In the case where $\alpha + 1 \geq 0$, Eq. (9) has a singularity at

$$a_c^{3(1+\alpha)} = 1 - \frac{B_s}{k' + B_s k}. \tag{16}$$

As in the previous case, to avoid a singularity in $0 < a < 1$, we have the conditions (i) $a_c > 1$ and (ii) $a_c < 0$. In each case, we divide the analysis into two parts: for $B_s > 0$ and for $B_s < 0$. In condition (i), the second term on the right side of Eq. (16) must be negative, which for $B_s > 0$, only occurs when $k' + B_s k < 0$. However, this condition never holds when $B_s > 0$. On the other hand, for $B_s < 0$, the second term on the right side of Eq. (16) is negative when $k' + B_s k > 0$, which is true if $-\frac{k'}{k} < B_S < 0$. Consequently, we identify another sub-region $\mathcal{N}_3 \subset \mathcal{M}$ with physical solutions, such that

$$\mathcal{N}_3 = \{(\alpha, B_s, k)/\alpha \geq -1, -\frac{k'}{k} < B_s < 0, 0 < k < 1\}. \tag{17}$$

At this point, it is worth mentioning that B_s being negative is not a problem. Unlike in other Chaplygin-like cosmologies where the first term in Eq. (1) has to be negative, in the CJG context this term can be positive while the third term is negative. The three

terms together can ensure the negativity of the entire expression in Eq. (1). Additionally, notice that for early times, i.e., $a \ll 1$, we have that

$$\rho \to \rho_i \equiv \rho_0 \left(\frac{-B_s k}{k'} \right)^{\frac{1}{1+\alpha}}, \tag{18}$$

which is perfectly compatible with negative values for B_s. Moreover, for $B_s > 0$, condition (ii) is satisfied when $0 < k' + B_s k < B_s$, which is the case for $B_s > 1$. However, positive values are not allowed by the limit in Eq. (18). Finally, for $B_s < 0$, condition (ii) is satisfied when $B_s < k' + B_s k < 0$, which is valid for $B_s < -\frac{k'}{k}$. Therefore, we also have physical solutions in the sub-region $\mathcal{N}_4 \subset \mathcal{M}$ such that

$$\mathcal{N}_4 = \{(\alpha, B_s, k) / \alpha > -1, B_s < -\frac{k'}{k}, 0 < k < 1\}. \tag{19}$$

Summarizing, we have physical solutions in

$$\mathcal{N} = \mathcal{N}_1 \cup \mathcal{N}_2 \cup \mathcal{N}_3 \cup \mathcal{N}_4. \tag{20}$$

We remark that the density is always positive in $\mathcal{N}$. Additionally, unlike CG, GCG, MCG, NCG, and VCG, the limit in the past for CJG (Eqs. (14) and (18)) does not correspond to a matter component. This implies that CJG cannot be used as a unified model.

B. Conditions for cosmic slowing down

The cosmic acceleration is usually attributed to the dominance of a negative pressure component. For instance, in the ΛCDM case, where $p = -\rho$, the pressure is always negative and acceleration will extend forever, driving the universe towards a dS phase as a final state. The same fate is predicted by GCG and other Chaplygin-like models. However, for the CJG model, depending on contributions to the pressure, this can be less negative, thereby opening the possibility of a decelerating phase immediately after the present accelerating phase. Consequently, it is interesting to check the existence of transient acceleration in the sub-region $\mathcal{N}$. To this end, we need to start with the following expressions for the deceleration parameter and for the relation between the Hubble function and a general EoS parameter $w(z)$

$$q(z) = -1 + \frac{1+z}{E} \frac{dE}{dz}, \qquad E^2(z) \propto \exp \left[3 \int_0^z \frac{1 + w(z')}{1 + z'} dz' \right]. \tag{21}$$

where $E(z) = H(z)/H_0$ and $H = \frac{\dot{a}}{a}$ is the Hubble rate. A transition between accelerated and decelerated phases requires a switch to a negative slope in the deceleration parameter, i.e., $\frac{dq}{dz} < 0$. Using Eqs. (21), it is possible to express this condition in terms of the EoS parameter (see [58] for details). This leads to the conclusion that slowing down acceleration requires at least the following condition to be met [58]:

$$\frac{dw}{dz} < 0. \tag{22}$$

Clearly, the ΛCDM and wCDM models do not predict cosmic slowing down [58]. Similarly, the GCG, MCG, and NGC models also predict a final dS phase for the universe, unlike the CJG model. Thus, we need to determine under which conditions a different fate from the dS phase will occur in the studied model.

The EoS parameter w as a function of the scale parameter can be found using Eqs. (4) and (9), which results in

$$w = -1 + \frac{(1 - B_s)k}{k(1 - B_s) + (k' + B_s k)a^{3(1+\alpha)}} + \frac{(1 - B_s)k'}{(k' + B_s k)a^{3(1+\alpha)} - (1 - B_s)k'}. \tag{23}$$

In the appendix, we present a detailed evaluation of the condition in Eq. (22). The results indicate that cosmic slowing down is possible in $\mathcal{N}_1$ and $\mathcal{N}_4$.

III. COSMOLOGY OF THE CJG

Here we study a cosmological model based on the results from the previous section using the CJG fluid as the DE component. First, we assume the cosmic substratum is dynamically dominated by a mixture of radiation (r), pressureless dark matter (m)

and a DE component (de). Radiation and matter are modeled by barotropic fluids with EoS parameters $w_r = 1/3$ and $w_m \ll 1$, respectively. The DE energy component is modeled as a CJG fluid with EoS (1).

In General Relativity, the Friedmann equation for a homogeneous, isotropic, and spatially flat three-component universe is

$$3H^2 = 8\pi\, G(\rho_r + \rho_m + \rho_{de})\,. \tag{24}$$

Here, ρ_r, ρ_m, and ρ_{de} are the radiation, pressureless dark matter, and DE densities, respectively. Moreover, energy conservation is satisfied by all the components separately

$$\dot{\rho}_i + 3H(\rho_i + p_i) = 0\,, \tag{25}$$

where $i = r, m, de$. As it is well-known, solutions of Eq. (25) for radiation and matter are found to be $\rho_r = \rho_{r0}a^{-4}$ and $\rho_m = \rho_{m0}a^{-3}$, respectively. For DE, the solution is given by Eq. (9). The sub-index "0" denotes the current value of any given quantity.

The past evolution is restricted by the necessity of a radiation and matter-dominated epochs to guarantee, for instance, the Big Bang Nucleosynthesis (BBN) and cosmic structure formation. To be a viable DE model, the CJG must be subdominant in the past, reproducing correctly a radiation domination era and subsequently, the matter domination era giving a decelerating universe. In recent times, the DE fluid must dominate to give rise the accelerating stage of the universe. A fluid with EoS given by (1) and within a subspace of parameters $\mathcal{N}$ reproduces all these points properly, as can be observed in Fig. 1 (left side), where the fractional densities are shown as a function of redshift. In all cases, the blue curves represent radiation, the red ones represent matter, and the black curves represent DE fluid. For the dot-dashed curve, parameter values are $\Omega_{m0} = 0.30$, $\alpha = 0.1$, $B_s = -0.6$, $k = 0.43$, corresponding to a point in $\mathcal{N}_3$. For the solid line, we used $\Omega_{m0} = 0.30$, $\alpha = 1.3$, $B_s = -1.4$, $k = 0.46$, corresponding to a point in $\mathcal{N}_4$. For the sake of comparison, we also plotted the corresponding functions in the ΛCDM model using the same colored dashed curves.
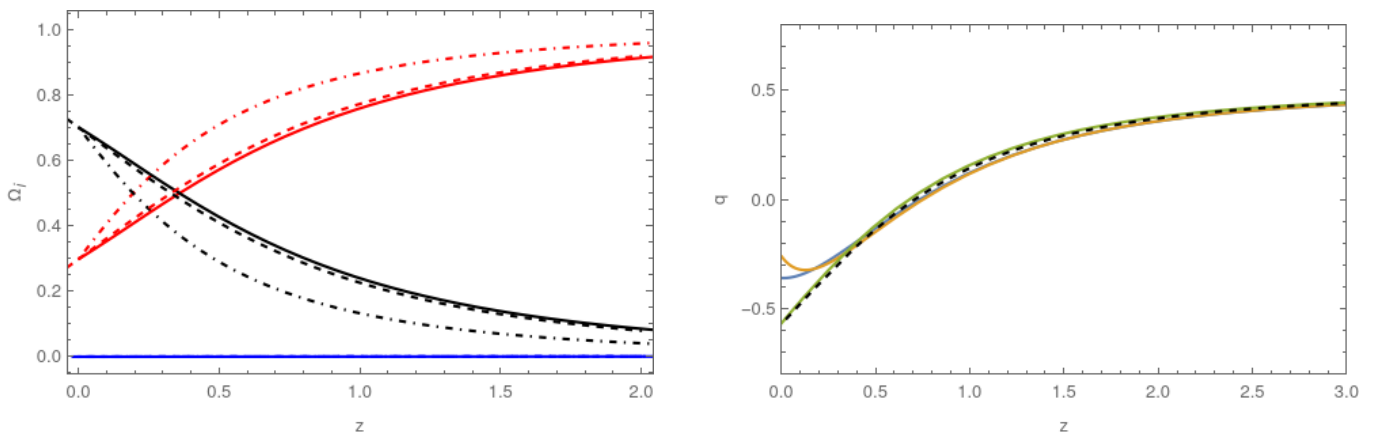

FIG. 1. Fractional densities for radiation, matter and DE (left) and deceleration parameter (right) as functions of redshift for different sets of parameters in the sub-region $\mathcal{N}$ (described in the text) for CJG and ΛCDM cosmologies.

On the other hand, the Hubble rate can be written as a function of the scale factor a. However, it will be more useful to have the dimensionless Hubble rate as a function of z

$$E^2(z) = \Omega_{r0}(1+z)^4 + \Omega_{m0}(1+z)^3 + (1 - \Omega_{m0} - \Omega_{r0})\left[B_s + \frac{B_s(1-B_s)(1+z)^{3(1+\alpha)}}{(k' + B_s\,k) - (1-B_s)k'(1+z)^{3(1+\alpha)}}\right]^{\frac{1}{1+\alpha}}, \tag{26}$$

where we have used the fact that each energy density is usually expressed in terms of the dimensionless density parameter, defined as $\Omega_i = \rho_i/\rho_{cr}$ with $\rho_{cr} = 3H^2/(8\pi G)$ being the critical density.

Having obtained the analytical expression for $E(z)$, we may proceed to analyze our model using the statefinder diagnostic. It will be useful to express thee Statefinder parameters in terms of the dimensionless Hubble rate and the redshift z. The cosmic times derivatives are written as redshift derivatives according to

$$\frac{d}{dt} = \frac{d}{dz}\frac{dz}{da}\frac{da}{dt} = -(1+z)H(z)\frac{d}{dz}\,.$$

In this way, the set of Statefinder parameters becomes

$$r = 1 + \frac{1}{2E^2}\left[(1+z)^2 \frac{d^2 E^2}{dz^2} - 2(1+z)\frac{dE^2}{dz}\right], \tag{27}$$

$$s = \frac{1}{3}\frac{(1+z)^2 \frac{d^2 E^2}{dz^2} - 2(1+z)\frac{dE^2}{dz}}{(1+z)\frac{dE^2}{dz} - 3E^2}. \tag{28}$$

Accordingly, upon replacement of Eq. (26) into Eqs. (27)-(28), the specific expressions for the Statefinder parameters are obtained (not shown), and they will be plotted in Section V using the best-fit values. Furthermore, we compute the effective EoS parameter w_{eff} for our CJG cosmological model, which encodes information about the universe's composition, the evolution of its energy density and the dynamics of its expansion. The general expression for w_{eff} depends on the first derivative of $E^2(z)$ with respect to the redshift z as follows

$$w_{eff} = -1 + \frac{1+z}{3E^2}\frac{dE^2}{dz}. \tag{29}$$

Thus, by replacing Eq.(26) into (29), w_{eff} for our specific CJG model is found (not shown).

As discussed above, for a universe dominated only by a CJG, a particular region in the subspace of parameters allows for transient acceleration-deceleration in the future. This feature must remain when a more realistic model of the universe is considered, including radiation and dark matter. Therefore, the future cosmological evolution within the framework of CJG may be very different from a dS. This is shown in Fig. 1 (right side), where several curves for deceleration parameter as a function of redshift were plotted for different sets of parameters. The dashed dark curve on the right side of Fig. 1 represents the case for ΛCDM, in which, as it is known, the accelerated expansion will continue forever. The green curve, which corresponds to the set $\Omega_m = 0.3$, $\alpha = 1.1$, $B_s = -0.81$ and $k = 0.55$, also indicates an eternal accelerated expansion. However, the last two curves, the blue one for $\Omega_m = 0.3$, $\alpha = 0.1$, $B_s = -1.5$, and $k = 0.43$, and the orange one for $\Omega_m = 0.3$, $\alpha = 0.8$, $B_s = -1.41$, and $k = 0.42$, exhibit a transition between an accelerated and a decelerated phase in the future. In all the curves, the transition from a decelerated evolution during the matter-dominated epoch to an accelerating phase in the past can be observed.

The possibility of future transient acceleration is not new. In the past, evidence was found for a slowing down of the expansion rate of the universe, or equivalently, for an increase in the deceleration parameter at redshifts close to the present epoch $z \approx 0$ [59, 63–68]. More recently, this possibility has been explored in light of recent data [60–62, 69, 70]. In fact, over the last few years, several authors have discussed the possibility that the accelerated expansion might be a transient phenomenon, i.e., that there might be a transition back to decelerated expansion [71–73].

So far, we have explored the concept of cosmic slowing down with a CJG fluid from a theoretical standpoint. However, in recent years, a large amount of cosmological data has emerged enabling very precise statistical tests. In the next section, we will use different probes to study the viability of a CJG as dark energy and what the data can tell us about the cosmic slowing down in the CJG framework. In this regard, several quantities describing the background evolution, such as the Hubble rate, the deceleration parameter, and the statefinder parameters, will be evaluated after obtaining the best-fit values from the aforementioned observational analysis.

IV. DATA

In Section II, the regions in the parameter space where the model has physical solutions were limited by imposing physical conditions on the fluid density (9). In this section, we will utilize current observational data to estimate the free parameters and their associated error bars. Through this process, we aim to determine the region in the parameter space where a model based on CJG could be compatible with observations. We will utilize cosmic chronometers (CC), Type Ia Supernovae (SNIa), Fast Gamma Ray Bursts (FRBs), and Baryon Acoustic Oscillations (BAO) datasets, along with their joint analysis, to perform a MCMC study. Implementations were carried out using the publicly available Python package `Polychord` [74]. Now, let us briefly describe each of the datasets used.

A. Cosmic Chronometers

The Hubble rate is the quantity that most directly characterizes the expansion of the universe. Over the last few years, its measurement has advanced significantly, and currently, there are two well-known methods to obtain $H(z)$ data. The first method utilizes the differential age of galaxies and is referred to as cosmic chronometers (CC) [75–78]. The second method measures the peaks of the baryon acoustic oscillations (BAO) observing the typical acoustic scale in the line-of-sight direction [79–82]. The CC technique relies on measuring the age difference between two ensembles of passively evolving massive galaxies at slightly

different redshifts, from which one can determine the derivative of redshift with respect to cosmic time [75]. This method has the advantage of avoiding systematic errors that arise when measuring the absolute ages of individual galaxies, instead allowing the measurement of the relative age difference between them. In a homogeneous and isotropic universe, the Hubble rate and the derivative of redshift with respect to cosmic time are related by

$$H(z) = -\frac{1}{1+z}\frac{dz}{dt} \simeq -\frac{1}{1+z}\frac{\Delta z}{\Delta t}. \tag{30}$$

Since the CC method does not rely on a particular functional form of the expansion history or spatial geometry, it can be regarded as a model-independent method. On the other hand, the BAO approach is based on the relation between $H(z)$ and the comoving differential radial distance. This method requires knowledge of the comoving BAO scale (r_{BAO}), which is derived from CMB measurements. This fact makes this probe not entirely cosmology-independent, since typically, in the derivation of the sound horizon scale from CMB a cosmological model is assumed [83]. Therefore, in this work, we have chosen to use the 31 measurements of the Hubble parameter $H(z)$ via the CC method, compiled in [84].

To estimate the region of parameters compatible with the CC dataset, we need to evaluate the likelihood function

$$-2ln(\mathscr{L}_{\mathrm{CC}}) = \chi^2 = \Delta\vec{C}^T C_{\mathrm{CC}}^{-1}\Delta\vec{C}, \tag{31}$$

where the vector $\Delta\vec{C}$ is the difference between H_i, i.e. each of the individual measurements of the sample considered, and H^{theo}, the set of Hubble parameters calculated from Eq. (26). The inverse covariance matrix is given by C_{CC}^{-1}. Here, we employ the method introduced by [85] to simulate possible correlations among these data points. This involves introducing positive correlations to 20% of the dataset by randomly selecting off-diagonal elements into the covariance matrix while maintaining its symmetry. The magnitude of these elements is set to

$$C_{ij} = 0.5\sigma_i\sigma_j, \tag{32}$$

being $0.5\sigma_i\sigma_j$ the 1σ errors of the elements i and j.

B. SNIa

Type Ia supernovae (SNIa) constitute a distinct and significant class of stellar phenomena, emerging during the terminal phases of stellar evolution and culminating in a catastrophic explosion that disperses stellar material into the cosmos. Given that SNIa are exceptionally bright, they can be detected at large cosmological distances and are sufficiently common to be found in large numbers. In fact, they have been crucial for mapping the cosmic expansion of the universe. The evidence for the accelerated cosmic expansion came from SNIa data analysis [3, 4].

For the cosmological analysis, the SNIa light curves must be standardized [86] to correct variations in brightness and other factors. This standardization ensures that their luminosities can be used as reliable distance indicators through the distance modulus equation [87]

$$\mu = m_b + \alpha x_1 - \beta c - M_B, \tag{33}$$

where α and β are parameters that relate stretch x_1 and color c to luminosity. M_B and m_b are the fiducial magnitude and the light-curve amplitude of the supernova, respectively. With this data, the χ^2 method is applied:

$$-2ln(\mathscr{L}_{\mathrm{SNIa}}) = \chi^2 = \Delta\vec{D}^T C_{stat+syst}^{-1}\Delta\vec{D}, \tag{34}$$

being $C_{stat+syst}^{-1}$ the combined statistical and systematic covariance matrix, and $\vec{D}$, the vector related to the distance module residuals computed from

$$\Delta D_i = \mu_i - \mu_{model}(z_i). \tag{35}$$

Here, $\mu_{model}(z_i) = 5log(d_L(z_i)/10\ \mathrm{pc})$ is the theoretical distance modulus estimated from the host galaxy redshift and the luminosity distance d_L, which considering a spatially flat universe is given by

$$d_L(z) = (1+z)\,c\int_0^z \frac{z'}{H(z')}. \tag{36}$$

In this paper, we constrain the CJG cosmological parameters using the Pantheon+ dataset (PAN$^+$), which comprises 1624 data points (when decoupled from the 77 SNe in Cepheid hosts used in SH0ES collaboration to calibrate the absolute magnitude).

C. FRBs

Fast Radio Bursts (FRBs) are intense pulses in the radio spectrum originating from cosmological distances, characterized by an extremely short duration (a few milliseconds). In recent years, they have emerged as interesting complementary cosmological probes. Discovered in 2007 [88], hundreds of bursts have been reported so far. While their progenitors remain unknown (for some progenitor models, see e.g., [89–91]), 24 of them have been localized, allowing determination of their host galaxies and redshifts. In this study, we perform our calculations on a subset of these FRBs, compiled by [92], excluding the nearest FRB, named FRB200110E, as it carries little cosmological information. Given the current uncertainties in modeling the extragalactic components of pulses, certain parameter choices can result in non-physical negative values for the dispersion measure DM. Consequently, we exclude FRB181030 ($z = 0.0039$) and FRB210807 ($z = 0.12927$) from our sample, as their DMs are estimated to be negative based on the methodology outlined below [93].

An FRB pulse is dispersed by the intergalactic medium during its path to the observer, generating a time delay between different radio frequencies that compose the observed signal. This dispersion is quantified by the dispersion measure DM, which is related to the column density of free electrons n_e along the FRB line of sight l, weighted by redshift as

$$\mathrm{DM} = \int \frac{n_e}{(1+z)} dl. \tag{37}$$

From an observational point of view, the observed dispersion measure $\mathrm{DM_{obs}}$, is expected to have four different contributions, such that

$$\mathrm{DM_{obs}} = \mathrm{DM_{ISM}} + \mathrm{DM_{halo}} + \mathrm{DM_{IGM}} + \frac{\mathrm{DM_{host}}}{(1+z)}. \tag{38}$$

The first two terms come from the intergalactic medium, and the last two come from the extragalactic medium. $\mathrm{DM_{ISM}}$ corresponds to the Milky Way interstellar medium contribution, $\mathrm{DM_{halo}}$ is related to the Milky Way galactic halo, $\mathrm{DM_{IGM}}$ is the contribution from the intergalactic medium (IGM), which incorporates the cosmological dependence, and $\mathrm{DM_{host}}$ is the host galaxy component corrected with $(1+z)^{-1}$ to account for cosmological expansion for a given FRB source at redshift z. $\mathrm{DM_{ISM}}$ is calculated using galactic electron distribution models (NE2001 [94] or YMW16 [95]). Since recent works have claimed that the YMW16 model may overestimate $\mathrm{DM_{ISM}}$ at low Galactic latitudes [96], we use the NE2001 approach. $\mathrm{DM_{halo}}$ has been estimated to be in the interval $50 < \mathrm{DM_{halo}} < 100 \, \mathrm{pc.cm^{-3}}$ [97]. However, to be conservative, we assume $\mathrm{DM_{halo}} = 50 \, \mathrm{pc.cm^{-3}}$ as in, for example, [98].

The exact characteristics of the host environment and the exact contribution of $\mathrm{DM_{host}}$ for each FRB are still uncertain. Therefore, the estimation of $\mathrm{DM_{host}}$ considers a probabilistic approach. Following [99], we use the stochastic distribution

$$P(\mathrm{DM_{host}}) = N\left(\langle \mathrm{DM_{host}} \rangle, \sigma_{\mathrm{host}}^2\right), \tag{39}$$

where N is a normal distribution with a mean value $\langle \mathrm{DM_{host}} \rangle = 100(1 + z_{\mathrm{host}})^{-1} \mathrm{pc.cm^{-3}}$ and variance $\sigma_{\mathrm{host}} = 50(1 + z_{\mathrm{host}})^{-1} \mathrm{pc.cm^{-3}}$. On the other hand, the dominant contribution in Eq.(38) is due to $\mathrm{DM_{IGM}}$. Recently, cosmological simulations have shown that the distribution of $\mathrm{DM_{IGM}}$ is influenced by the distribution of baryons around galactic halos and the number of collapsed structures intersecting a given line of sight. Two different approaches have been used to take this influence into account: the non-Gaussian [92, 100, 101] and the Gaussian [99, 102, 103] approaches. In this work, we use the Gaussian approach; however, recent studies with the 23 localized FRB data points have shown that there is no appreciable difference between using either approaches [104]. The Gaussian approach assumes a normal distribution around the mean

$$\langle \mathrm{DM_{IGM}} \rangle = \frac{3c\,\Omega_{\mathrm{b}} H_0}{8\pi G m_{\mathrm{p}}} \int_0^z \frac{(1+z') f_{\mathrm{IGM}}(z') f_{\mathrm{e}}(z')}{E(z')} dz', \tag{40}$$

with standard deviation interpolated in the range $\sigma_{\mathrm{IGM}}(z=0) \approx 10 \, \mathrm{pc.cm^{-3}}$ and $\sigma_{\mathrm{IGM}}(z=1) \approx 400 \, \mathrm{pc.cm^{-3}}$. In Eq. (40), $f_{\mathrm{e}}(z) = Y_{\mathrm{H}} X_{\mathrm{e,H}}(z) + \frac{1}{2} Y_{\mathrm{He}} X_{\mathrm{e,He}}(z)$. The cosmic baryon density, the proton mass, and the fraction of baryon mass in the IGM are denoted as Ω_b, m_{p}, and f_{IGM}, respectively. Because both hydrogen and helium are completely ionized at $z < 3$, the ionization fractions of each species are $X_{\mathrm{e,H}} = X_{\mathrm{e,He}} = 1$. Additionally, we consider an IGM with a hydrogen mass fraction $Y_{\mathrm{H}} = 0.75$ and a helium mass fraction $Y_{\mathrm{He}} = 0.25$. Moreover, several analyses have found a constant value for the fraction of baryon mass, $f_{\mathrm{IGM}} = 0.82$ (see e.g., [104, 105]). Finally, in Eq. (38), $\mathrm{DM_{IGM}}$ is estimated by $\mathrm{DM_{IGM}} = \mathrm{DM_{obs}} - \mathrm{DM_{local}} - \mathrm{DM_{host}}(1+z)^{-1}$, with uncertainty given as

$$\sigma_{\mathrm{IGM}}(z) = \sqrt{\sigma_{\mathrm{obs}}(z)^2 + \sigma_{\mathrm{local}}^2 + \left(\frac{\sigma_{\mathrm{host}}(z)}{1+z}\right)^2}, \tag{41}$$

where σ_{obs} and σ_{host} are the errors related to DM_{obs} and DM_{host}, respectively. Meanwhile, σ_{local} is the sum of uncertainties in DM_{ISM} and DM_{halo}. Following [99], we approximate $\sigma_{local} \approx 30 \; pc.cm^{-3}$.

In order to compute the likelihood, we must consider that every observed dispersion measure DM_i at a given redshift z_i is related to a Gaussian individual likelihood through

$$\mathscr{L}(DM_i, z_i) = \frac{1}{\sqrt{2\pi\sigma_i^2}} \exp\left[\frac{\left(DM_i - DM^{theo}(z_i)\right)^2}{2\sigma_i^2}\right], \tag{42}$$

where $DM^{theo}(z_i)$ is the theoretical contribution computed as $DM^{theo}(z_i) = DM_{obs} - DM_{ISM} - DM_{halo} = DM_{IGM}(z_i) + DM_{host}(z_i)$, with

$$\sigma^2(z_i) = \sigma_{MW}^2 + \sigma_{host}^2(z_i) + \sigma_{IGM}^2(z_i). \tag{43}$$

Considering all events as independent, the total likelihood of the sample is

$$\mathscr{L}_{FRBs} = \prod_i \mathscr{L}_i, \tag{44}$$

and the computation of the product is executed for every the 23 FRB data points.

D. BAO

A key cosmological probe for investigating the LSS of the universe corresponds to the Baryonic Acoustic Oscillations (BAO). These oscillations, arising from waves in the photon-baryon fluid of the early universe, created distinct density fluctuations. As the universe expanded and cooled, these fluctuations left an imprint as a characteristic scale of approximately 150 Mpc in the matter distribution, most notably in the separation between galaxies. This scale serves as a "standard ruler" for measuring cosmic distances and the expansion rate of the universe.

BAO data is derived by analyzing the large-scale distribution of galaxy clusters, with measurements taken both transversely and radially to determine the angular diameter distance and the Hubble rate across various redshifts. These measurements play a significant role in constraining the expansion history of the universe. Large-scale surveys, such as the Sloan Digital Sky Survey (SDSS) [106], have mapped BAO signatures with remarkable precision.

To compare cosmological models with observational data, we consider the following key distance ratios:

$$\frac{d_m(z)}{r_d} = \frac{d_l(z)}{r_d(1+z)}, \tag{45}$$

being $d_m(z)$ is the transverse comoving distance, and r_d represents the sound horizon at the drag epoch. Throughout this analysis, we adopt the value of r_d determined by the latest Planck collaboration results [6]. Another fundamental quantity is the ratio

$$\frac{d_H(z)}{r_d} = \frac{c}{r_d H(z)}, \tag{46}$$

where $d_H(z)$ is the Hubble distance and $H(z)$ denotes the Hubble parameter. Finally, we consider the volume-averaged angular diameter distance, given by

$$\frac{d_v(z)}{r_d} = \frac{[z d_m^2(z) d_H(z)]^{1/3}}{r_d}. \tag{47}$$

This set of distance measures provides essential constraints for testing cosmological models against large-scale structure and BAO observations.

In this study, we use the most up-to-date release from the DESI collaboration, in which they provide BAO measurements combining DESI 2024 [107] galaxy and quasar BAO measurements with SDSS-BOSS and eBOSS results, to estimate the parameters of the models investigated in this work. In this case, the likelihood for each ratio $X = d_m/r_D$, d_H/r_D, d_v/r_D is given by

$$-2ln(\mathscr{L}_{BAO}) = \chi_{BAO}^2 = \sum_i^N \left\{ \left[\frac{X_i - X_{theo}}{\sigma_{X_i}}\right]^2 + \ln(2\pi\sigma_{X_i}^2) \right\}. \tag{48}$$

V. ANALYSES AND RESULTS

We have implemented two separate scenarios for the MCMC joint analysis: (a) CC + FRBs + BAO, which entirely excludes SNIa, and (b) CC + FRBs + BAO + PAN$^+$. In order to perform all analyses, we fixed $\Omega_r = 5.38 \times 10^{-5}$ to be consistent with CMB observations [108], and considered the following set of free parameters: $H_0, \Omega_m, \alpha, B_s,$ and k. For consistency, we used the same flat priors in all cases, such as $[20, 100]$ for H_0 and $[0, 1]$ for Ω_m. For $\alpha, B_s,$ and k, we suitably considered the sub-regions in $\mathcal{N}$. Moreover, when the additional parameter M_B is introduced, we used a flat prior of $[-20, -18]$.

Results for the (a) and (b) analyses are presented in Fig. 2 and Table I. Both analyses exhibit good agreement within the 1σ statistical confidence level (C.L.), indicating concordance between the CJG cosmology in the region $\mathcal{N}_3 \cup \mathcal{N}_4$ and observations. Their best-fit values support a slowing-down phase. In the contour plots of Fig. 2, it is possible to observe some general features. For example, in general, regions with $1 + \alpha > 0$ and $B_s < 0$ are preferred by observations; i.e. the data favor the $\mathcal{N}_3 \cup \mathcal{N}_4$ region, with a slight trend towards $\mathcal{N}_3$. This can be seen in Fig. 3 (left), where the plane B_s-k is shown together with the curve $B_s = -\frac{k'}{k}$ (black dashed curve) separating $\mathcal{N}_3$ (de Sitter future) and $\mathcal{N}_4$ (non-de Sitter future). Notice that the best-fit point indicated by x lies within the slowdown region. Moreover, there is a positive correlation between the B_s and k parameters, which can be explained by the k-dependence of the intervals for B_s (see Sec. II). Additionally, in Table I, we present the χ^2_{min} and χ^2_ν values, along with the Akaike Information Criterion (AIC) and Bayesian Information Criterion (BIC) values. The $\chi^2_\nu \sim 1$ for CJG in cases (a) and (b) indicates that the data are well fitted by the model.
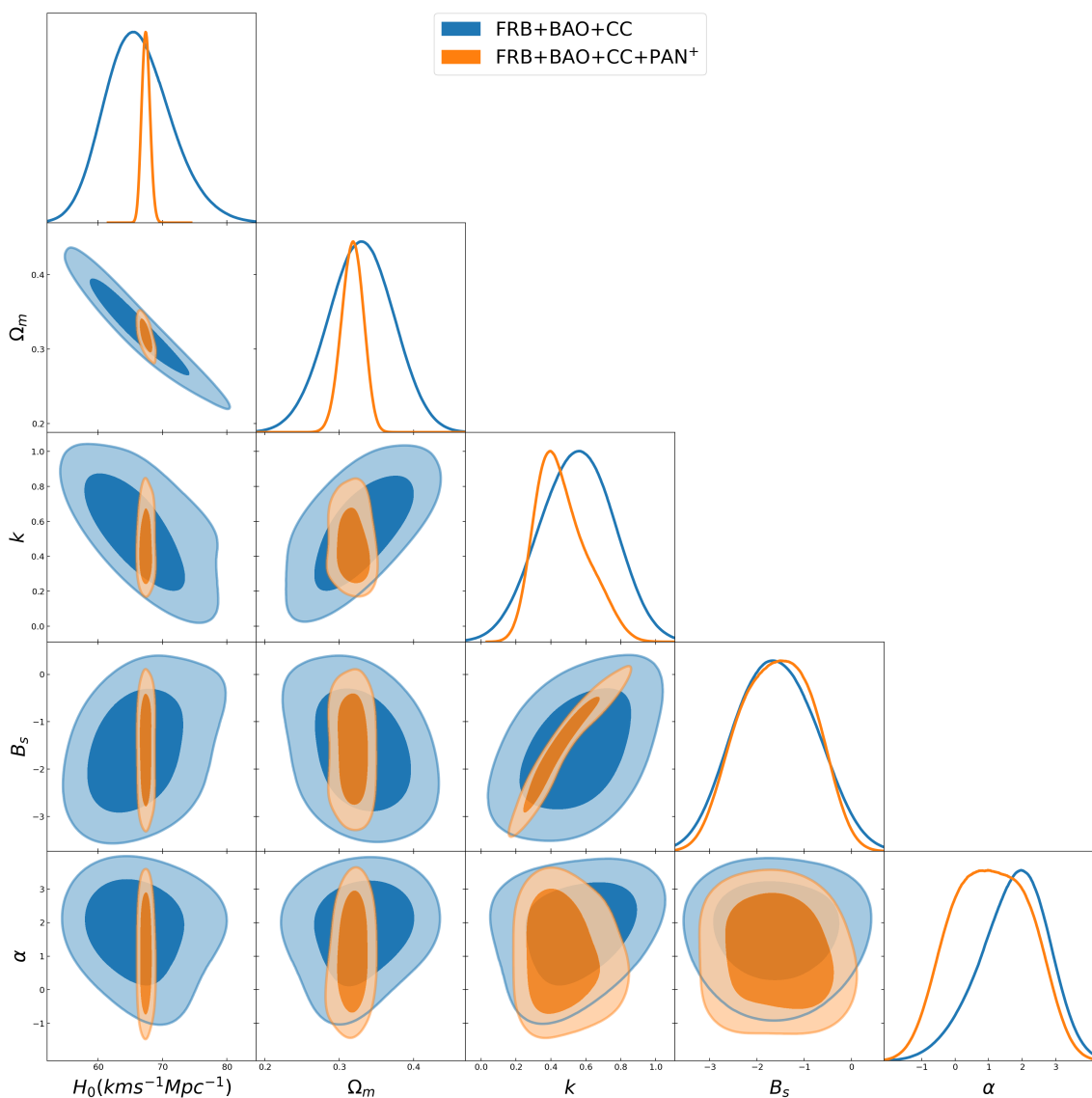

FIG. 2. 1σ and 2σ C.L. curves from the MCMC analysis for CJG using (a) FRBs + BAO + CC and (b) FRBs + BAO + CC + PAN$^+$.

With the best-fit values obtained from the joint analysis CC+FRBs+BAO+PAN$^+$ for example, we can plot relevant quantities that describe the cosmic evolution at the background level and compare them with those from the ΛCDM model. Fig. 3 (right) shows the plot of the relative deviation between the Hubble function of CJG and that of the ΛCDM model, $1-H_{CJG}(z)/H_{\Lambda CDM}$. As shown from Fig.3, $H(z)$ becomes indistinguishable for both models during the past, while it approaches very close values in the present time, resulting in a very small negative relative difference. In future times, $H(z)$ for CJG becomes smaller than that for the ΛCDM model, leading to a positive relative deviation. Conversely, cosmic acceleration is accounted for by the deceleration parameter, which is depicted in Fig. 4. As can be seen, the best-fit values (black curves) support cosmic deceleration in the future. These findings are interesting because they present a different behavior compared to the ΛCDM case (blue line on the left side of Fig.4) and other types of Chaplygin-like fluids such as NCG, MCG, and GCG, as shown on the right side of Fig.4[1]. Nevertheless, it is important to note that the 1σ region (gray region in Fig. 4) is relatively large and sufficiently inclusive to also encompass a dS final fate for the universe. In general, further data and analyses are needed to refine our understanding of the final fate of the universe

Model	Data	H_0	Ω_m	B_s	k	α	M_B	$\chi^2_{\min}$	χ^2_ν	AIC	BIC
CJG	(a)	$66.10^{+4.20}_{-5.40}$	0.329 ± 0.041	-1.60 ± 0.79	0.55 ± 0.20	$1.73^{+1.10}_{-0.75}$	-	55.11	1.04	67.11	79.57
	(b)	67.41 ± 0.62	0.318 ± 0.014	-1.57 ± 0.75	$0.46^{+0.08}_{-0.18}$	1.1 ± 1.1	$-19.423^{+0.018}_{-0.020}$	1623.85	0.97	1637.85	1675.83
ΛCDM	(a)	68.66 ± 0.89	0.306 ± 0.016	-	-	-	-	48.67	0.87	60.67	60.90
	(b)	67.56 ± 0.57	0.3296 ± 0.0097	-	-	-	-19.429 ± 0.016	1595.39	0.95	1607.39	1625.09

TABLE I. Best-fit values and their 1σ errors for (a) FRB + BAO + CC and (b) FRB + BAO + CC + PAN$^+$, for the CJG and ΛCDM models. We also include the $\chi^2_{\min}$, χ^2_ν, AIC, and BIC values.
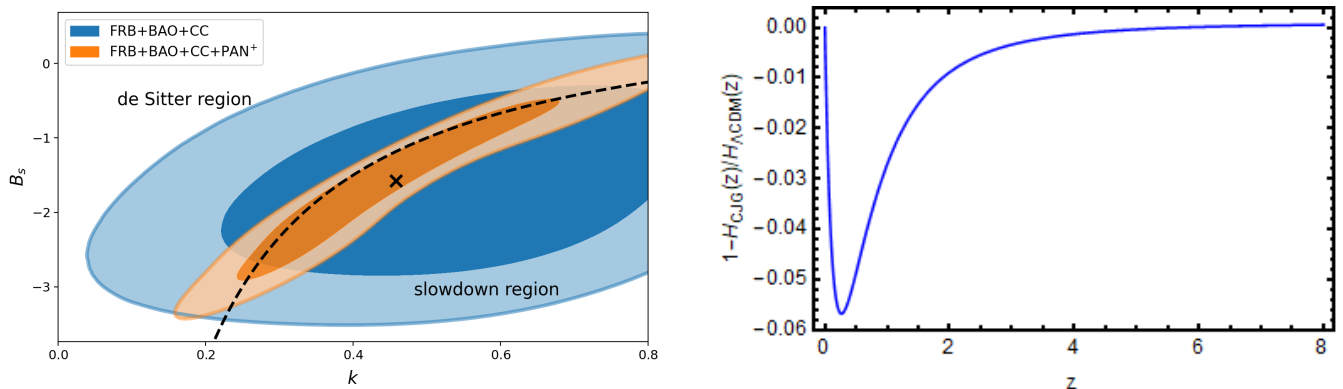

FIG. 3. Left: $B_s - k$ plane for the joint analysis, alongside the curve $B_S = -\frac{k'}{k}$ (black dashed curve), separating regions $\mathcal{N}_3$ and $\mathcal{N}_4$. Right: plot of the relative deviation between the Hubble function of CJG and that of the ΛCDM model, $1 - H_{CJG}(z)/H_{\Lambda CDM}$, using the best-fit parameters from (b) FRB + BAO + CC + PAN$^+$.

A complementary analysis is provided by the statefinder parameters r and s, which account for the deviations of the CJG model from ΛCDM. In Fig. 5 (left), the trajectory traced by the CJG in the $s - r$ plane is shown, obtained by parametrically plotting Eqs. (27) and (28) with varying z. If the role of DE is played by a cosmological constant, the value of r remains constant at $r = 1$ throughout the matter-dominated epoch and into the future (for $z \lesssim 10^4$). In the $s - r$ plane, the fixed point $\{s, r\} = \{0, 1\}$ corresponds to the Λ CDM case. For the CJG case, at past times ($z > 0$), the pair (s, r) is $\sim (0, 1)$, indistinguishable from ΛCDM. However, currently, the parameters are $s \simeq 8$ and $r \simeq -6$, indicating a deviation of the CJG trajectory from ΛCDM. In Fig. 5 (right) the effective EoS parameter w_{eff} (29) is displayed. The solid-black and solid-blue lines correspond to the CJG and ΛCDM models, respectively. The effective EoS parameter w_{eff} provides a summary of the combined effects of various components in the universe. As observed, w_{eff} changes during the matter-dominated and dark-energy-dominated epochs, reflecting the dominant component's EoS parameter at that time. For CJG and ΛCDM, the effective EoS parameters are practically indistinguishable in the past. However, around the present epoch, in CJG case, w_{eff} starts to increase and at some point in the future it becomes positive, indicating cosmic deceleration. This corroborates the late-time behavior of CJG initially observed from the deceleration parameter (Fig. 5).

---

[1] To plot the deceleration curve for Chaplygin-like models, we used the best-fit values for NCG, MCG, and GCG found in [48]
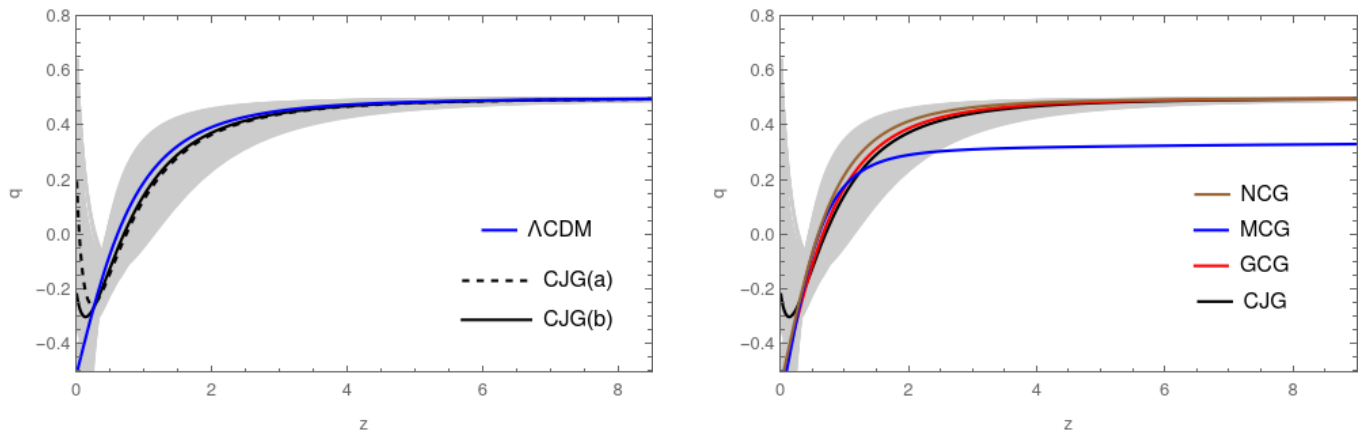
FIG. 4. Deceleration parameter as a function of redshift for the best-fit values found in the joint analysis (b) FRBs + BAO + CC + PAN$^+$ (continuous black curve) alongside its 1σ region, together with the best-fit for (a) FRBs + BAO + CC (dashed black curve) and ΛCDM case (left) and other Chaplygin-type cases (right).
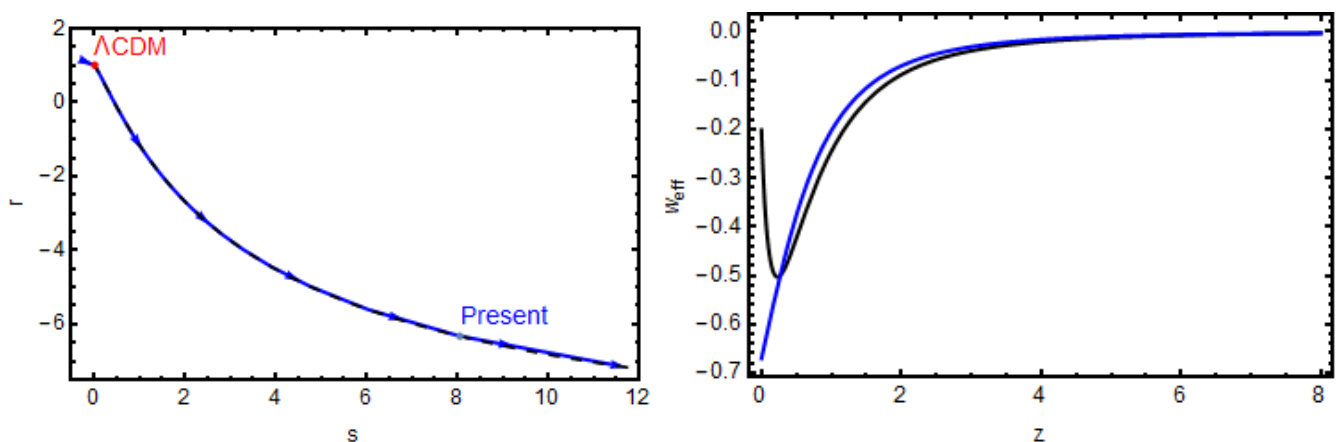

FIG. 5. Plots of the trajectory on the $s-r$ plane for the statefinder analysis (left panel) and the evolution of the effective EoS parameter against z for the CJG cosmological model. For both plots, we have used the best fit parameters found in the analysis (b) FRB + BAO + CC + PAN$^+$.

VI. CONCLUSIONS AND FINAL REMARKS

We have explored an extension of the Chaplygin EoS, derived from a specific generalization of the Chaplygin inflationary model within the framework of the Hamilton-Jacobi formalism and elliptic functions [49]. By imposing conditions to obtain physical solutions for the energy density, we reduced the parameter space to different sub-regions where the model is free of singularities within the interval $0 < a < 1$, and the density remains always positive. Interestingly, two of these sub-regions are compatible with the possibility of a new deceleration phase in the future, following the current acceleration. Then, we used different data samples such as SNIa, CC, FRBs and BAO to investigate the viability of the CJG cosmological model including radiation and matter. Constraints on the free parameters we obtained using a statistical MCMC analyses and their error bars are presented in Table I. Best-fit values for joint analyses (a) and (b)support: the cosmic slowing down phenomenon (see Fig. **??**) with a maximum of acceleration at $z \sim 0.02$, α values such that $\alpha + 1 > 0$ and negative values for B_s, with a $\chi^2_\nu \sim 1$. The preference for negative values for the B_s parameter implies a lack of direct correspondence with the GCG. Additionally, the best-fit values result in a cosmology almost indistinguishable from ΛCDM in the past, deviating from it only in recent epoch, and diverging from the eternal dS expansion.

Exploring CJG expands two families of models. Firstly, it increases the number of models within the Chaplygin type family. Unlike other models in this family, however, CJG allows for a future acceleration-deceleration transition. Secondly, it enlarges the family of models that predict future deceleration, such as interacting models, w parametrizations, decaying dark matter, extensions of quintessential cosmology, and others (see, for example, [59, 61, 63, 70], and references therein). Moreover, it has been observed that a potential future transition to a decelerating stage, thereby naturally ending the eternal accelerating regime, is significant from a physical perspective [70]. An eternal de Sitter phase disagrees with the requirements of the S-matrix

describing particle interactions and can be problematic within the framework of string theory [109–111]. Our model comparison with ΛCDM yields $\Delta\chi^2_{\min} \sim 6.4$ for case (a) and $\Delta\chi^2_{\min} \sim 28.5$ for case (b), indicating strong and very strong evidence for ΛCDM, respectively. Regarding the information criteria, ΔAIC ~ 6.4, and ΔBIC ~ 18.7 for case (a). Following Jeffreys' scale [112], this suggests strong evidence (ΔAIC) and very strong evidence (ΔBIC) for ΛCDM. For case (b), we find ΔAIC ~ 30.5, and ΔBIC ~ 50.7, providing very strong evidence against CJG. However, it is important to emphasize that these results are inherently model-dependent. A definitive understanding of the universe's ultimate fate may require a model-independent, fully data-driven approach, opening opportunities for future research.

[1] A. Einstein, "The foundation of the general theory of relativity.," *Annalen Phys.*, vol. 49, no. 7, pp. 769–822, 1916.

[2] K. N. Abazajian *et al.*, "Inflation Physics from the Cosmic Microwave Background and Large Scale Structure," *Astropart. Phys.*, vol. 63, pp. 55–65, 2015.

[3] A. G. Riess *et al.*, "Observational evidence from supernovae for an accelerating universe and a cosmological constant," *Astron. J.*, vol. 116, pp. 1009–1038, 1998.

[4] S. Perlmutter *et al.*, "Measurements of Ω and Λ from 42 high redshift supernovae," *Astrophys. J.*, vol. 517, pp. 565–586, 1999.

[5] D. N. Spergel *et al.*, "First year Wilkinson Microwave Anisotropy Probe (WMAP) observations: Determination of cosmological parameters," *Astrophys. J. Suppl.*, vol. 148, pp. 175–194, 2003.

[6] N. Aghanim *et al.*, "Planck 2018 results. VI. Cosmological parameters," *Astron. Astrophys.*, vol. 641, p. A6, 2020. [Erratum: Astron.Astrophys. 652, C4 (2021)].

[7] R. J. Cooke, M. Pettini, and C. C. Steidel, "One percent determination of the primordial deuterium abundance," *The Astrophysical Journal*, vol. 855, no. 2, p. 102, 2018.

[8] D. J. Eisenstein *et al.*, "Detection of the Baryon Acoustic Peak in the Large-Scale Correlation Function of SDSS Luminous Red Galaxies," *Astrophys. J.*, vol. 633, pp. 560–574, 2005.

[9] T. Padmanabhan, "Cosmological constant: The Weight of the vacuum," *Phys. Rept.*, vol. 380, pp. 235–320, 2003.

[10] V. Sahni and A. A. Starobinsky, "The Case for a positive cosmological Lambda term," *Int. J. Mod. Phys. D*, vol. 9, pp. 373–444, 2000.

[11] S. M. Carroll, "The Cosmological constant," *Living Rev. Rel.*, vol. 4, p. 1, 2001.

[12] S. Weinberg, "The Cosmological Constant Problem," *Rev. Mod. Phys.*, vol. 61, pp. 1–23, 1989.

[13] J. Martin, "Everything You Always Wanted To Know About The Cosmological Constant Problem (But Were Afraid To Ask)," *Comptes Rendus Physique*, vol. 13, pp. 566–665, 2012.

[14] I. Zlatev, L.-M. Wang, and P. J. Steinhardt, "Quintessence, cosmic coincidence, and the cosmological constant," *Phys. Rev. Lett.*, vol. 82, pp. 896–899, 1999.

[15] N. Arkani-Hamed, L. J. Hall, C. F. Kolda, and H. Murayama, "A New perspective on cosmic coincidence problems," *Phys. Rev. Lett.*, vol. 85, pp. 4434–4437, 2000.

[16] E. Di Valentino, O. Mena, S. Pan, L. Visinelli, W. Yang, A. Melchiorri, D. F. Mota, A. G. Riess, and J. Silk, "In the realm of the Hubble tension—a review of solutions," *Class. Quant. Grav.*, vol. 38, no. 15, p. 153001, 2021.

[17] A. G. Riess, S. Casertano, W. Yuan, J. B. Bowers, L. Macri, J. C. Zinn, and D. Scolnic, "Cosmic Distances Calibrated to 1% Precision with Gaia EDR3 Parallaxes and Hubble Space Telescope Photometry of 75 Milky Way Cepheids Confirm Tension with ΛCDM," *Astrophys. J. Lett.*, vol. 908, no. 1, p. L6, 2021.

[18] E. Di Valentino *et al.*, "Cosmology Intertwined III: $f\sigma_8$ and S_8," *Astropart. Phys.*, vol. 131, p. 102604, 2021.

[19] E. J. Copeland, M. Sami, and S. Tsujikawa, "Dynamics of dark energy," *Int. J. Mod. Phys. D*, vol. 15, pp. 1753–1936, 2006.

[20] S. Nojiri and S. D. Odintsov, "Introduction to modified gravity and gravitational alternative for dark energy," *eConf*, vol. C0602061, p. 06, 2006.

[21] T. Clifton, P. G. Ferreira, A. Padilla, and C. Skordis, "Modified Gravity and Cosmology," *Phys. Rept.*, vol. 513, pp. 1–189, 2012.

[22] K. Bamba, S. Capozziello, S. Nojiri, and S. D. Odintsov, "Dark energy cosmology: the equivalent description via different theoretical models and cosmography tests," *Astrophys. Space Sci.*, vol. 342, pp. 155–228, 2012.

[23] A. Joyce, L. Lombriser, and F. Schmidt, "Dark Energy Versus Modified Gravity," *Ann. Rev. Nucl. Part. Sci.*, vol. 66, pp. 95–122, 2016.

[24] N. Bilic, G. B. Tupper, and R. D. Viollier, "Unification of dark matter and dark energy: The Inhomogeneous Chaplygin gas," *Phys. Lett. B*, vol. 535, pp. 17–21, 2002.

[25] M. Heydari-Fard and H. R. Sepangi, "Generalized Chaplygin gas as geometrical dark energy," *Phys. Rev. D*, vol. 76, p. 104009, 2007.

[26] R. Jackiw, "A Particle field theorist's lectures on supersymmetric, nonAbelian fluid mechanics and d-branes," 10 2000.

[27] A. Y. Kamenshchik, U. Moschella, and V. Pasquier, "An Alternative to quintessence," *Phys. Lett. B*, vol. 511, pp. 265–268, 2001.

[28] J. C. Fabris, S. V. B. Goncalves, and P. E. De Souza, "Mass power spectrum in a universe dominated by the Chaplygin gas," *Gen. Rel. Grav.*, vol. 34, pp. 2111–2126, 2002.

[29] V. Gorini, A. Kamenshchik, and U. Moschella, "Can the Chaplygin gas be a plausible model for dark energy?," *Phys. Rev. D*, vol. 67, p. 063509, 2003.

[30] M. C. Bento, O. Bertolami, and A. A. Sen, "Generalized Chaplygin gas, accelerated expansion and dark energy matter unification," *Phys. Rev. D*, vol. 66, p. 043507, 2002.

[31] W. S. Hipolito-Ricaldi, H. E. S. Velten, and W. Zimdahl, "Non-adiabatic dark fluid cosmology," *JCAP*, vol. 06, p. 016, 2009.

[32] W. S. Hipolito-Ricaldi, H. E. S. Velten, and W. Zimdahl, "The Viscous Dark Fluid Universe," *Phys. Rev. D*, vol. 82, p. 063507, 2010.

[33] W. Zimdahl, H. E. S. Velten, and W. S. Hipolito-Ricaldi, "Viscous dark fluid Universe: a unified model of the dark sector?," *Int. J. Mod. Phys. Conf. Ser.*, vol. 3, pp. 312–323, 2011.

[34] F. Perrotta, S. Matarrese, and M. Torki, "Instability of chaplygin gas trajectories in unified dark matter models," *Phys. Rev. D*, vol. 70, p. 121304, Dec 2004.

[35] M. Biesiada, W. Godłowski, and M. Szydłowski, "Generalized Chaplygin Gas Models Tested with Type Ia Supernovae," *Astrophys. J.*, vol. 622, pp. 28–38, Mar. 2005.

[36] R. Colistete, Jr. and J. C. Fabris, "Bayesian analysis of the (generalized) Chaplygin gas and cosmological constant models using the 157 gold SNe Ia data," *Class. Quant. Grav.*, vol. 22, pp. 2813–2834, 2005.

[37] Z.-H. Zhu, "Generalized Chaplygin gas as a unified scenario of dark matter/energy: Observational constraints," *Astron. Astrophys.*, vol. 423, pp. 421–426, 2004.

[38] P. Wu and H. W. Yu, "Generalized Chaplygin gas model: Constraints from Hubble parameter versus redshift data," *Phys. Lett. B*, vol. 644, pp. 16–19, 2007.

[39] M. Makler, S. Quinet de Oliveira, and I. Waga, "Constraints on the generalized Chaplygin gas from supernovae observations," *Phys. Lett. B*, vol. 555, p. 1, 2003.

[40] S. del Campo and J. R. Villanueva, "Observational Constraints on the Generalized Chaplygin Gas," *Int. J. Mod. Phys. D*, vol. 18, pp. 2007–2022, 2009.

[41] H. Sandvik, M. Tegmark, M. Zaldarriaga, and I. Waga, "The end of unified dark matter?," *Phys. Rev. D*, vol. 69, p. 123524, 2004.

[42] R. F. vom Marttens, L. Casarini, W. Zimdahl, W. S. Hipólito-Ricaldi, and D. F. Mota, "Does a generalized Chaplygin gas correctly describe the cosmological dark sector?," *Phys. Dark Univ.*, vol. 15, pp. 114–124, 2017.

[43] H. Benaoum, "Accelerated Universe from Modified Chaplygin Gas and Tachyonic Fluid," *Universe*, vol. 8, no. 7, p. 340, 2022.

[44] U. Debnath, A. Banerjee, and S. Chakraborty, "Role of modified Chaplygin gas in accelerated universe," *Class. Quant. Grav.*, vol. 21, pp. 5609–5618, 2004.

[45] X. Zhang, F.-Q. Wu, and J. Zhang, "A New generalized Chaplygin gas as a scheme for unification of dark energy and dark matter," *JCAP*, vol. 01, p. 003, 2006.

[46] X.-H. Zhai, Y.-D. Xu, and X.-Z. Li, "Viscous generalized Chaplygin gas," *Int. J. Mod. Phys. D*, vol. 15, pp. 1151–1162, 2006.

[47] A. Hernández-Almada, M. A. García-Aspeitia, M. A. Rodríguez-Meza, and V. Motta, "A hybrid model of viscous and Chaplygin gas to tackle the Universe acceleration," *Eur. Phys. J. C*, vol. 81, no. 4, p. 295, 2021.

[48] J. Zheng, S. Cao, Y. Lian, T. Liu, Y. Liu, and Z.-H. Zhu, "Revisiting Chaplygin gas cosmologies with the recent observations of high-redshift quasars," *Eur. Phys. J. C*, vol. 82, no. 7, p. 582, 2022.

[49] J. R. Villanueva, "The generalized Chaplygin-Jacobi gas," *JCAP*, vol. 07, p. 045, 2015.

[50] W. S. Hipólito-Ricaldi and J. R. Villanueva, "A Jacobian generalization of the pseudo-Nambu–Goldstone boson potential," *Int. J. Mod. Phys. D*, vol. 26, no. 03, p. 1750019, 2016.

[51] A. Gallego Cadavid and J. R. Villanueva, "No slow-roll inflation à la generalized Chaplygin gas in general relativity," *JCAP*, vol. 12, p. 044, 2020.

[52] U. Debnath, "Roles of modified Chaplygin–Jacobi and Chaplygin–Abel gases in FRW universe," *Int. J. Mod. Phys. A*, vol. 36, no. 33, p. 2150245, 2021.

[53] P. Mukherjee, U. Debnath, and A. Pradhan, "Accretion of modified Chaplygin–Jacobi gas and modified Chaplygin–Abel gas onto Schwarzschild black hole," *Int. J. Geom. Meth. Mod. Phys.*, vol. 20, no. 12, p. 2350218, 2023.

[54] H. Chaudhary, U. Debnath, T. Roy, S. Maity, G. Mustafa, and M. Arora, "Constraints on the parameters of modified Chaplygin-Jacobi and modified Chaplygin-Abel gases in $f(T)$ gravity," ArXiv: 2307.14691.

[55] M. Fathi, J. R. Villanueva, G. Aguilar-Pérez, and M. Cruz, "Black hole in a generalized Chaplygin–Jacobi dark fluid: Shadow and light deflection angle," *Phys. Dark Univ.*, vol. 46, p. 101598, 2024.

[56] V. Sahni, T. D. Saini, A. A. Starobinsky, and U. Alam, "Statefinder: A New geometrical diagnostic of dark energy," *JETP Lett.*, vol. 77, pp. 201–206, 2003.

[57] U. Alam, V. Sahni, T. D. Saini, and A. A. Starobinsky, "Exploring the expanding universe and dark energy using the Statefinder diagnostic," *Mon. Not. Roy. Astron. Soc.*, vol. 344, p. 1057, 2003.

[58] M.-J. Zhang and J.-Q. Xia, "Physical condition for the slowing down of cosmic acceleration," *Nucl. Phys. B*, vol. 929, pp. 438–451, 2018.

[59] C. Z. Vargas, W. S. Hipolito-Ricaldi, and W. Zimdahl, "Perturbations for transient acceleration," *JCAP*, vol. 04, p. 032, 2012.

[60] Y. Hu, M. Li, N. Li, and S. Wang, "A comprehensive investigation on the slowing down of cosmic acceleration," *Astrophys. J.*, vol. 821, no. 1, p. 60, 2016.

[61] J. Magaña, V. H. Cárdenas, and V. Motta, "Cosmic slowing down of acceleration for several dark energy parametrizations," *JCAP*, vol. 10, p. 017, 2014.

[62] Y. L. Bolotin, V. A. Cherkaskiy, M. I. Konchatnyi, S. Pan, and W. Yang, "Do current observations support transient acceleration of our universe?," *Int. J. Mod. Phys. D*, vol. 31, no. 05, p. 2250036, 2022.

[63] A. Shafieloo, V. Sahni, and A. A. Starobinsky, "Is cosmic acceleration slowing down?," *Phys. Rev. D*, vol. 80, p. 101301, 2009.

[64] A. C. C. Guimarães and J. A. S. Lima, "Could the cosmic acceleration be transient? A cosmographic evaluation," *Classical and Quantum Gravity*, vol. 28, p. 125026, June 2011.

[65] R.-G. Cai and Z.-L. Tuo, "Detecting the cosmic acceleration with current data," *Phys. Lett. B*, vol. 706, pp. 116–122, 2011.

[66] F. E. M. Costa and J. S. Alcaniz, "Cosmological consequences of a possible Λ-dark matter interaction," *Phys. Rev. D*, vol. 81, p. 043506, Feb. 2010.

[67] J. C. Fabris, B. Fraga, N. Pinto-Neto, and W. Zimdahl, "Transient cosmic acceleration from interacting fluids," *JCAP*, vol. 04, p. 008, 2010.

[68] W. Zimdahl, C. Z. Vargas, and W. S. Hipólito-Ricaldi, "Interacting dark energy and transient accelerated expansion," in *13th Marcel Grossmann Meeting on Recent Developments in Theoretical and Experimental General Relativity, Astrophysics, and Relativistic Field Theories*, pp. 1577–1579, 2015.

[69] M. Shahalam, S. Sami, and A. Agarwal, "Om diagnostic applied to scalar field models and slowing down of cosmic acceleration," *Mon. Not. Roy. Astron. Soc.*, vol. 448, no. 3, pp. 2948–2959, 2015.

[70] A. A. Escobal, J. F. Jesus, S. H. Pereira, and J. A. S. Lima, "Can the Universe decelerate in the future?," *Phys. Rev. D*, vol. 109, no. 2, p. 023514, 2024.

[71] A. Albrecht and C. Skordis, "Phenomenology of a realistic accelerating universe using only Planck scale physics," *Phys. Rev. Lett.*, vol. 84, pp. 2076–2079, 2000.

[72] J. Barrow, R. Bean, and J. Magueijo, "Can the universe escape eternal acceleration?," *Mon. Not. Roy. Astron. Soc.*, vol. 316, p. L41, 2000.

[73] M. C. Bento, O. Bertolami, and N. M. C. Santos, "A Two field quintessence model," *Phys. Rev. D*, vol. 65, p. 067301, 2002.

[74] W. Handley, M. Hobson, and A. Lasenby, "Polychord: nested sampling for cosmology," *Monthly Notices of the Royal Astronomical Society: Letters*, vol. 450, no. 1, pp. L61–L65, 2015.

[75] R. Jimenez and A. Loeb, "Constraining cosmological parameters based on relative galaxy ages," *Astrophys. J.*, vol. 573, pp. 37–42, 2002.

[76] D. Stern, R. Jimenez, L. Verde, M. Kamionkowski, and S. A. Stanford, "Cosmic chronometers: constraining the equation of state of dark energy. I: H(z) measurements," *JCAP*, vol. 2010, p. 008, Feb. 2010.

[77] C. Zhang, H. Zhang, S. Yuan, S. Liu, T.-J. Zhang, and Y.-C. Sun, "Four new observational H(z) data from luminous red galaxies in the Sloan Digital Sky Survey data release seven," *Research in Astronomy and Astrophysics*, vol. 14, pp. 1221–1233, Oct. 2014.

[78] M. Moresco, L. Pozzetti, A. Cimatti, R. Jimenez, C. Maraston, L. Verde, D. Thomas, A. Citro, R. Tojeiro, and D. Wilkinson, "A 6% measurement of the Hubble parameter at $z \sim 0.45$: direct evidence of the epoch of cosmic re-acceleration," *JCAP*, vol. 05, p. 014, 2016.

[79] E. Gaztanaga, A. Cabre, and L. Hui, "Clustering of Luminous Red Galaxies IV: Baryon Acoustic Peak in the Line-of-Sight Direction and a Direct Measurement of H(z)," *Mon. Not. Roy. Astron. Soc.*, vol. 399, pp. 1663–1680, 2009.

[80] N. G. Busca *et al.*, "Baryon Acoustic Oscillations in the Ly-α forest of BOSS quasars," *Astron. Astrophys.*, vol. 552, p. A96, 2013.

[81] A. Font-Ribera *et al.*, "Quasar-Lyman α Forest Cross-Correlation from BOSS DR11 : Baryon Acoustic Oscillations," *JCAP*, vol. 05, p. 027, 2014.

[82] T. Delubac *et al.*, "Baryon acoustic oscillations in the Lyα forest of BOSS DR11 quasars," *Astron. Astrophys.*, vol. 574, p. A59, 2015.

[83] K. Jiao, N. Borghi, M. Moresco, and T.-J. Zhang, "New Observational H(z) Data from Full-spectrum Fitting of Cosmic Chronometers in the LEGA-C Survey," *Astrophys. J. Suppl.*, vol. 265, no. 2, p. 48, 2023.

[84] G.-J. Wang, X.-J. Ma, S.-Y. Li, and J.-Q. Xia, "Reconstructing functions and estimating parameters with artificial neural networks: A test with a hubble parameter and sne ia," *The Astrophysical Journal Supplement Series*, vol. 246, no. 1, p. 13, 2020.

[85] L. Kazantzidis and L. Perivolaropoulos, "Evolution of the fσ8 tension with the planck 15/λ cdm determination and implications for modified gravity theories," *Physical Review D*, vol. 97, no. 10, p. 103503, 2018.

[86] L. Amendola and S. Tsujikawa, *Dark energy: theory and observations*. Cambridge University Press, 2010.

[87] D. Brout, D. Scolnic, B. Popovic, A. G. Riess, A. Carr, J. Zuntz, R. Kessler, T. M. Davis, S. Hinton, D. Jones, *et al.*, "The pantheon+ analysis: cosmological constraints," *The Astrophysical Journal*, vol. 938, no. 2, p. 110, 2022.

[88] D. R. Lorimer, M. Bailes, M. A. McLaughlin, D. J. Narkevic, and F. Crawford, "A bright millisecond radio burst of extragalactic origin," *Science*, vol. 318, no. 5851, pp. 777–780, 2007.

[89] C. D. Bochenek, V. Ravi, K. V. Belov, G. Hallinan, J. Kocz, S. R. Kulkarni, and D. L. McKenna, "A fast radio burst associated with a galactic magnetar," *Nature*, vol. 587, no. 7832, pp. 59–62, 2020.

[90] B. Zhang, "The physical mechanisms of fast radio bursts," *Nature*, vol. 587, no. 7832, pp. 45–53, 2020.

[91] S. Bhandari, E. M. Sadler, J. X. Prochaska, S. Simha, S. D. Ryder, L. Marnoch, K. W. Bannister, J.-P. Macquart, C. Flynn, R. M. Shannon, *et al.*, "The host galaxies and progenitors of fast radio bursts localized with the australian square kilometre array pathfinder," *The Astrophysical Journal Letters*, vol. 895, no. 2, p. L37, 2020.

[92] K. Yang, Q. Wu, and F. Wang, "Finding the missing baryons in the intergalactic medium with localized fast radio bursts," *The Astrophysical Journal Letters*, vol. 940, no. 2, p. L29, 2022.

[93] J. A. S. Fortunato, D. J. Bacon, W. S. Hipólito-Ricaldi, and D. Wands, "Fast Radio Bursts and Artificial Neural Networks: a cosmological-model-independent estimation of the Hubble constant," *JCAP*, vol. 01, p. 018, 2025.

[94] J. M. Cordes and T. J. W. Lazio, "Ne2001. i. a new model for the galactic distribution of free electrons and its fluctuations," *arXiv preprint astro-ph/0207156*, 2002.

[95] J. Yao, R. Manchester, and N. Wang, "A new electron-density model for estimation of pulsar and frb distances," *The Astrophysical Journal*, vol. 835, no. 1, p. 29, 2017.

[96] S. K. Ocker, J. M. Cordes, and S. Chatterjee, "Constraining Galaxy Halos from the Dispersion and Scattering of Fast Radio Bursts and Pulsars," *Astrophys. J.*, vol. 911, p. 102, Apr. 2021.

[97] J. X. Prochaska and Y. Zheng, "Probing galactic haloes with fast radio bursts," *Monthly Notices of the Royal Astronomical Society*, vol. 485, no. 1, pp. 648–665, 2019.

[98] J.-P. Macquart, J. Prochaska, M. McQuinn, K. Bannister, S. Bhandari, C. Day, A. Deller, R. Ekers, C. James, L. Marnoch, *et al.*, "A census of baryons in the universe from localized fast radio bursts," *Nature*, vol. 581, no. 7809, pp. 391–395, 2020.

[99] S. Hagstotz, R. Reischke, and R. Lilow, "A new measurement of the hubble constant using fast radio bursts," *Monthly Notices of the Royal Astronomical Society*, vol. 511, no. 1, pp. 662–667, 2022.

[100] J. X. Prochaska, S. Simha, C. Law, N. Tejos, *et al.*, "Frbs/frb: First doi release of this repository," *Zenodo*, 2019.

[101] Q. Wu, H. Yu, and F. Wang, "A new method to measure hubble parameter h (z) using fast radio bursts," *The Astrophysical Journal*, vol. 895, no. 1, p. 33, 2020.

[102] M. Jaroszynski, "Fast radio bursts and cosmological tests," *Monthly Notices of the Royal Astronomical Society*, vol. 484, no. 2, pp. 1637–1644, 2019.

[103] J.-G. Zhang, Z.-W. Zhao, Y. Li, J.-F. Zhang, D. Li, and X. Zhang, "Cosmology with fast radio bursts in the era of ska," *arXiv preprint arXiv:2307.01605*, 2023.

[104] J. A. S. Fortunato, W. S. Hipólito-Ricaldi, and M. V. dos Santos, "Cosmography from well-localized fast radio bursts," *Mon. Not. Roy. Astron. Soc.*, vol. 526, no. 2, pp. 1773–1782, 2023.

[105] J. M. Shull, B. D. Smith, and C. W. Danforth, "The baryon census in a multiphase intergalactic medium: 30% of the baryons may still be missing," *The Astrophysical Journal*, vol. 759, no. 1, p. 23, 2012.

[106] K. Accetta, C. Aerts, V. S. Aguirre, R. Ahumada, N. Ajgaonkar, N. F. Ak, S. Alam, C. A. Prieto, A. Almeida, F. Anders, *et al.*, "The seventeenth data release of the sloan digital sky surveys: Complete release of manga, mastar, and apogee-2 data," *The Astrophysical Journal Supplement Series*, vol. 259, no. 2, p. 35, 2022.

[107] A. Adame, J. Aguilar, S. Ahlen, S. Alam, D. Alexander, M. Alvarez, O. Alves, A. Anand, U. Andrade, E. Armengaud, *et al.*, "Desi 2024 iii: Baryon acoustic oscillations from galaxies and quasars," *arXiv preprint arXiv:2404.03000*, 2024.

[108] P. A. Zyla *et al.*, "Review of Particle Physics," *PTEP*, vol. 2020, no. 8, p. 083C01, 2020.

[109] W. Fischler, A. Kashani-Poor, R. McNees, and S. Paban, "The Acceleration of the universe, a challenge for string theory," *JHEP*, vol. 07, p. 003, 2001.

[110] J. M. Cline, "Quintessence, cosmological horizons, and self-tuning," *Journal of High Energy Physics*, vol. 2001, p. 035, Aug. 2001.

[111] S. Hellerman, N. Kaloper, and L. Susskind, "String theory and quintessence," *JHEP*, vol. 06, p. 003, 2001.

[112] A. R. Liddle, "Information criteria for astrophysical model selection," *Mon. Not. Roy. Astron. Soc.*, vol. 377, pp. L74–L78, 2007.

Appendix A: Sub-region for cosmic slowing down

In this appendix, we present a detailed computation of the condition for having cosmic slowing down of the current acceleration. First, we consider the EoS parameter for the CJG model as a function of redshift

$$\omega(z) = -1 + \frac{(1 - B_s)k}{k(1 - B_s) + (k' + B_s k)(1 + z)^{-3(1+\alpha)}} + \frac{(1 - B_s)k'}{(k' + B_s k)(1 + z)^{-3(1+\alpha)} - (1 - B_s)k'} \,. \tag{A1}$$

Next, we use the change of variable $y = \rho^{1+\alpha}$ in Eq. (4). The EoS parameter and its derivative as functions of the new variable are

$$w = -\frac{B_s k}{y} - 2k' + \frac{k'}{B_s}y, \qquad \frac{dw}{dy} = \frac{B_s k}{y^2} + \frac{k'}{B_s} \,. \tag{A2}$$

Considering the y variable, the condition for cosmic deceleration (22) can be written as

$$\frac{dw}{dz} = \frac{dw}{dy}\frac{dy}{dz} < 0 \,. \tag{A3}$$

For $B_s < 0$, $\frac{dw}{dy}$ is always negative, so $\frac{dy}{dz}$ must be always positive. In other words,

$$\frac{dy}{dz} = 3(1+\alpha)B_s(1 - B_s)\frac{(k' + B_s k)(1 + z)^{-1-3(1+\alpha)}}{[(k' + B_s k)(1 + z)^{-3(1+\alpha)} - (1 - B_s)k']^2} > 0 \tag{A4}$$

Then, this last condition reduces to

$$(1 + \alpha)(k' + B_s k) < 0 \,. \tag{A5}$$

In the case $\alpha + 1 \geq 0$, this is valid for $B_s < -\frac{k'}{k}$.

For $B_s > 0$, $\frac{dw}{dy}$ is always positive, and then condition (A4) reduces to

$$(1 + \alpha)(1 - B_s) < 0 \tag{A6}$$

$\alpha + 1 < 0$, this condition is valid when $B_s > 1$. Therefore, the CJG presents cosmic slowdown in $\mathcal{N}_1$ and $\mathcal{N}_4$.